A Reflectarray With Low Profile Based on the Method of Choosing the Certain Phase Constant

Wenting Li, *Member, IEEE*, Wenting Lin, Ruiyang Li, Yejun He, *Senior Member, IEEE*, Yao Gao, Chong Zhang, *Member, IEEE*, and Steven Gao, *Fellow, IEEE*

***Abstract*—In this letter, a reflectarray antenna with a small focal diameter ratio (F/D) is presented. It is found that when the F/D is extremely small, the phase constant used in calculating the required reflection phase on the reflecting surface significantly affects the radiation pattern. In certain cases, an unsuitable phase constant can even cause the main beam to split. The unit cell is implemented as a stacked patch, and the reflecting surface comprises 14 × 14 elements. The effect of the phase constant on the radiation pattern is analyzed, and two reflectarrays with phase constants of 90° and 180°, both operating at 10 GHz with an F/D of 0.05, are compared. These two reflectarrays are simulated, fabricated, and measured. The measured results show good agreement with the simulations. Within the operating band, the reflectarray with a phase constant of 90° achieves a maximum measured gain of 20.42 dBi, with the first sidelobe level (SLL1) below −10 dB. The radiation pattern of the reflectarray with a phase constant of 180° is totally distorted, resulting in a measured gain of 6.56 dBi at 10 GHz and an SLL1 of −5.8 dB.**

***Index Terms*—Low profile, phase constant, reflectarrays.**

I. Introduction

COMPARED with traditional phased arrays, reflectarrays typically have a larger profile, which is determined by their feeding mechanism [1]. For elements on the reflecting surface, the incident angle of electromagnetic (EM) waves increases as the profile decreases, which alters the performance of these elements [2]. This constraint limits profile reduction. If the distance between the feed antenna and the reflecting surface is forcibly reduced without special design considerations, the radiation pattern may become distorted, and the gain could decrease.

Researchers have proposed different methods to reduce the profile of reflectarrays. One effective approach is the use of folded reflectarrays. In [3], [4], and [5], the transmitarray is applied as the polarizer in folded reflectarrays, effectively reducing the antenna's physical profile. In [6] and [7], a grid polarizer is used to construct a folded reflectarray. In [8], a folded reflectarray is realized by utilizing a metal grid, which acts as the polarizer. In [9], a spherical polarizer instead of a flat one is employed to build a folded reflectarray. In [10], a circularly polarized selective surface is used as a polarizer to design the folded reflectarray. In [11], a Cassegrain reflectarray with a subreflector is proposed. Apart from reducing the profile by applying folded reflectarrays, researchers have also analyzed the performance of reflectarray elements under large electromagnetic wave incident angles. In [12] and [13], the forced linked boundary condition (FLBC) allows for calculating the reflection phase of elements at large incident angles. In [14], a reflectarray with an F/D of 0.117 is designed, where the reflection phase is calculated using a 7 × 7 reflecting surface illuminated by a plane wave.

In this letter, an ultralow-profile reflectarray is proposed, in which the feed antenna is implemented as a waveguide. Stacked patches are used as the unit cells to build the reflecting surface. When calculating the required reflection phase of the unit cell on the reflecting surface, an adjustable constant is added. The effect of the phase constant on the radiation pattern of the reflectarray is analyzed, and by selecting an appropriate phase constant, a reflectarray with an F/D of 0.05 is realized. The resulting reflectarray exhibits stable radiation patterns. In this design, as the reflecting surface is square, D is the length of its sides. To the best of the authors' knowledge, the proposed reflectarray achieves the smallest F/D among all low-profile reflectarrays reported.

II. Design of the Low-Profile Reflectarray

In this section, a low-profile reflectarray operating at 10 GHz is designed. The structure of the elements on the reflecting surface is described, and a detailed analysis of the phase constant's effect on the radiation pattern is provided.

A. Unit Cell

The unit cell applied in the proposed reflectarray is the stacked patch, as shown in Fig. 1. Each unit cell is composed of two substrates separated by an air layer. The thickness of the air layer is $t2$. Two patches are printed on the top surfaces of the substrates (Rogers 4003C), each with a thickness of $t1$. The Rogers 4003C has a relative permittivity of 3.55 and a loss tangent of 0.0027. The dimensions of the top patch are 0.8 times those of the bottom patch. The size of the element is $L \times L$. The dimension of the bottom patch is $W \times C$. The reflection phase of the element is controlled by varying W. As W changes from 3 mm to 13 mm, the

Received 12 December 2024; revised 20 January 2025; accepted 27 January 2025. Date of publication 4 February 2025; date of current version 4 June 2025. This work was supported in part by the National Key Research and Development Program of China under Grant 2023YFE0107900 and in part by the National Natural Science Foundation of China under Grant 62101341 and Grant 62071306. *(Corresponding author: Ruiyang Li.)*

Wenting Li, Wenting Lin, and Yejun He are with the State Key Laboratory of Radio Frequency Heterogeneous Integration, School of Electronic and Information Engineering, Shenzhen University, Shenzhen 518000, China.

Ruiyang Li is with the School of Electrical and Information Engineering, Zhengzhou University, Zhengzhou 450000, China (e-mail: ruiyangnpu@gmail.com).

Yao Gao is with the School of Information Engineering, Chang'an University, Xi'an 710000, China.

Chong Zhang is with the School of Information Science and Engineering, Shenyang University of Technology, Shenyang 710000, China.

Steven Gao is with the Department of Electronic Engineering, Chinese University of Hong Kong, Hong Kong, China.

Digital Object Identifier 10.1109/LAWP.2025.3537993

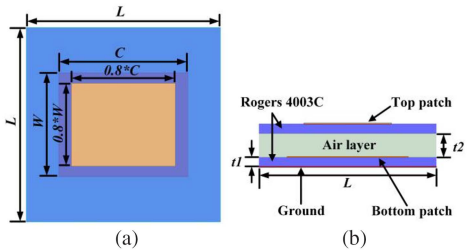

Fig. 1. Geometry of the unit cell. (a) Top view. (b) Front view.

TABLE I
PARAMETERS OF THE REFLECTARRAY ELEMENT (UNIT: MM)

Parameter	L	C	$t1$	$t2$
Value	15	10	0.813	2

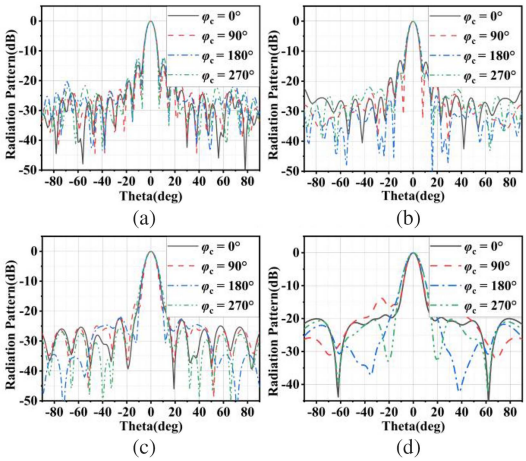

Fig. 2. Radiation patterns with different φ_c values when F/D is (a) 0.85, (b) 0.5, (c) 0.289, and (d) 0.134.

reflection phase varies from 0° to −557°. The parameter values of the element are shown in Table I.

B. Phase Calculation

In the traditional reflectarray theory, the required phase of each element on the reflecting surface is given by [15], [16], [17]

$$\varphi\ (x_{mn}, y_{mn}) = -k_0 \sin\theta_b\,(x_{mn}\cos\phi_b + y_{mn}\sin\phi_b) + k_0 R_{mn} + \varphi_c \quad (1)$$

where (x_{mn}, y_{mn}) is the coordinate of the element and R_{mn} is the distance between the phase center of the feed and the element. k_0 is the wave number in free space. The direction of the required beam is $(\theta_b, \emptyset_b)$. φ_c is a constant.

Theoretically, φ_c does not affect the radiation patterns of the reflectarray and can take any value. This applies to reflectarrays with a relatively large F/D. Fig. 2 shows the radiation patterns of reflectarrays with different F/D values as φ_c changes. These results are obtained via full-wave simulation. In Fig. 2(a) and (b), it is evident that when F/D is larger than 0.5, the radiation patterns are almost not affected by φ_c.

However, as the F/D decreases, φ_c begins to affect the radiation patterns of the reflectarray. In Fig. 2(c), it can be seen that the beamwidth of the main beam changes slightly as φ_c varies.

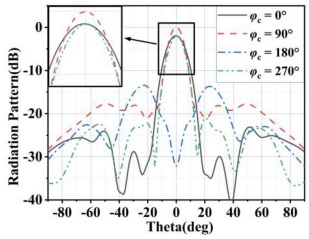

Fig. 3. Radiation patterns with different φ_c values when F/D is 0.05.

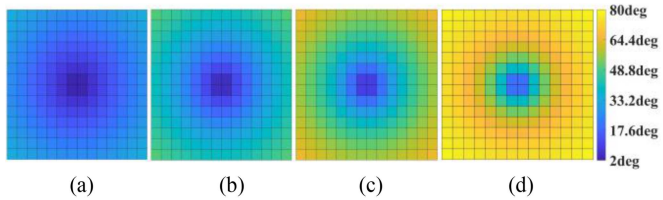

Fig. 4. Incident angles for the element on the reflecting surface when F/D is (a) 0.85, (b) 0.5, (c) 0.289, and (d) 0.134.

In Fig. 2(d), when F/D is 0.134, the SLL1 is approximately −20 dB, with φ_c being 270°. However, it increases to −14 dB when φ_c is 90°.

To demonstrate the effects of φ_c when F/D is extremely small, the radiation patterns of the reflectarray with the F/D of 0.05 are shown in Fig. 3. With such a small F/D, the radiation patterns are significantly influenced by φ_c. The radiation patterns keep stable when φ_c is 0°, 90°, and 270°. However, the main beam of the reflectarray splits completely when φ_c is 180°. In this case, the directivity decreases by approximately 13 dB, and the SLL1 deteriorates dramatically.

This phenomenon can be attributed to two main factors. First, when F/D is very small, the incident angle for each element on the reflecting surface varies substantially. Fig. 4 shows the incident angles on the reflecting surface for different F/D values. In Fig. 4(a), most incident angles range from 15° to 20°, with the largest angle being 30°. The largest incident angles are 45° and 60°, respectively, in Fig. 4(b) and (c). In Fig. 4(d), with the F/D being 0.134, most incident angles range from 50° to 70°, with the maximum angle being 75°. For certain elements, it is evident that smaller F/D values correspond to larger incident angles. When the incident angle becomes sufficiently large, the reflection phase of the element varies with changes in the incident angle [18]. Although the FLBC proposed in [12] provides a method to analyze the reflection phase of elements with arbitrary incident angles, it gives the reflection phase only when the incident angle is less than 60°.

The second reason is that when F/D is very small, the incident angles of adjacent elements differ significantly, causing partial disruption of the periodic boundary conditions of the element on the reflecting surface. Fig. 5(a) shows the directivity and SLL1 for different φ_c values when F/D is 0.05. As φ_c increases from 0° to 270°, SLL1 initially increases and then decreases. The highest SLL1 reaches −9.55 dB, which occurs when φ_c is 180°. The highest directivity is 21.35 dBi, which is achieved when φ_c is 90°, and the lowest directivity, 7.93 dBi, is observed when φ_c is 180°. These results indicate that φ_c affects the radiation patterns, directivity, and SLL1 of the reflectarray when F/D is very small.

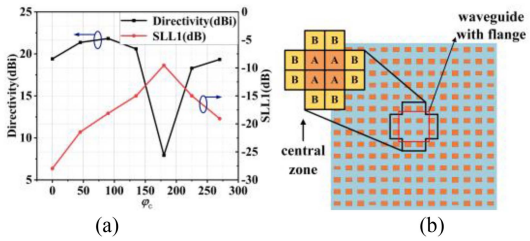

Fig. 5. (a) Directivity and SLL1 with different values of φ_c when F/D is 0.05. (b) Positions of type A and B elements.

TABLE II
PARAMETERS COMPARISON OF THE CENTRAL ZONE ELEMENT WITH DIFFERENT φ_c

φ_c (deg)	W_A (mm)	W_B (mm)	Directivity (dBi)
0	7.4	6.1	19.41
90	6.8	8.2	21.35
180	4.9	7.6	7.93
270	7.9	7.1	19.34

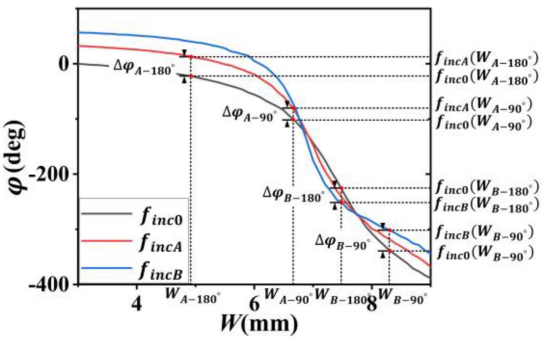

Fig. 6. Positions of type A and B elements on the phase shift curve with different incident angles, with φ_c being 90° and 180°.

The elements in the central zone of the reflecting surface are analyzed, as these elements receive more EM energy from the feed antenna compared with those outside the central zone. In this zone, there are 12 elements, which are classified into types A and B, as shown in Fig. 5(b). Type A elements are surrounded by type B elements.

Table II gives the dimensions of type A and B elements, as well as the directivity of the reflectarray for different φ_c values when F/D is 0.05. W_A is the W of type A elements while W_B is the W of type B elements. Table II shows when φ_c is 90°, the directivity is the highest. When φ_c is 180°, the radiation pattern is completely distorted, and the directivity decreases to 7.93 dBi. When φ_c is 0° and 270°, the directivity drops by approximately 2 dB compared to that when φ_c is 90°. Therefore, in the design of reflectarrays with small F/D, φ_c being 180° should be avoided.

To explain the effect of φ_c on the radiation pattern, type A and B elements are analyzed, as they are located in the central zone and receive more EM energy from the feed antenna compared to elements outside this zone. The positions of type A and B elements are shown in Fig. 5(b). The positions of type A and B elements on the phase shift curve with different incident angles are shown in Fig. 6. The reflection phase curve of the element is different under different incident angles. f_{inc0} is the reflection phase curve when the incident angle is 0°. f_{incA} and f_{incB} are the reflection phase curves with the incident angles for type A and B elements, respectively. In this design, $incA$ and $incB$ are 55° and 72.5°, respectively. When calculating the required reflection phase on the reflecting surface, the incident angle of the element is assumed to be 0°. The required phase difference $\Delta\varphi$ between type A and B elements is given by

$$\Delta\varphi = f_{inc0}\left(W_{A-\varphi_c}\right) - f_{inc0}\left(W_{B-\varphi_c}\right) \tag{2}$$

where $f_{inc0}(W_{A-\varphi_c})$ is the reflection phase corresponding to $W_{A-\varphi_c}$ for type A elements with an incident angle of 0° and $f_{inc0}(W_{B-\varphi_c})$ is the reflection phase for type B elements.

However, the practical phase difference $\Delta\varphi'$ between type A and B elements is given by

$$\Delta\varphi' = f_{incA}\left(W_{A-\varphi_c}\right) - f_{incB}\left(W_{B-\varphi_c}\right) \tag{3}$$

where $incA$ and $incB$ are the incident angles for type A and B elements. Since $\Delta\varphi$ and $\Delta\varphi'$ are different, the difference between $\Delta\varphi$ and $\Delta\varphi'$ is represented by $\Delta\varepsilon$, which is given by

$$\Delta\varepsilon = \Delta\varphi' - \Delta\varphi = \Delta\varphi_{A-\varphi_c} - \Delta\varphi_{B-\varphi_c} \tag{4}$$

where

$$\begin{cases} \Delta\varphi_{A-\varphi_c} = f_{incA}\left(W_{A-\varphi_c}\right) - f_{inc0}\left(W_{A-\varphi_c}\right) \\ \Delta\varphi_{B-\varphi_c} = f_{incB}\left(W_{B-\varphi_c}\right) - f_{inc0}\left(W_{B-\varphi_c}\right) \end{cases}. \tag{5}$$

$\Delta\varepsilon$ is determined by $\Delta\varphi_{A-\varphi_c}$ and $\Delta\varphi_{B-\varphi_c}$. $\Delta\varphi_{A-\varphi_c}$ and $\Delta\varphi_{B-\varphi_c}$ are related to φ_c. Therefore, $\Delta\varepsilon$ is also related to φ_c.

Different φ_c values lead to different $\Delta\varepsilon$ values. The larger $\Delta\varepsilon$ is, the greater the error between the practical phase difference and the calculated phase difference. Therefore, $\Delta\varepsilon$ should be as small as possible.

The absolute value of $\Delta\varepsilon$ is given by

$$|\Delta\varepsilon| = \begin{cases} \left||\Delta\varphi_{A-\varphi_c}| - |\Delta\varphi_{B-\varphi_c}|\right|, \Delta\varphi_{A-\varphi_c}\cdot\Delta\varphi_{B-\varphi_c} > 0 \\ \left||\Delta\varphi_{A-\varphi_c}| + |\Delta\varphi_{B-\varphi_c}|\right|, \Delta\varphi_{A-\varphi_c}\cdot\Delta\varphi_{B-\varphi_c} < 0 \end{cases}. \tag{6}$$

From Fig. 6, it can be seen that

$$\begin{cases} \Delta\varphi_{A-90^\circ} = f_{incA}\left(W_{A-90^\circ}\right) - f_{inc0}\left(W_{A-90^\circ}\right) > 0 \\ \Delta\varphi_{B-90^\circ} = f_{incB}\left(W_{B-90^\circ}\right) - f_{inc0}\left(W_{B-90^\circ}\right) > 0 \\ \Delta\varphi_{A-180^\circ} = f_{incA}\left(W_{A-180^\circ}\right) - f_{inc0}\left(W_{A-180^\circ}\right) > 0 \\ \Delta\varphi_{B-180^\circ} = f_{incB}\left(W_{B-180^\circ}\right) - f_{inc0}\left(W_{B-180^\circ}\right) < 0 \end{cases}. \tag{7}$$

Therefore, when φ_c are 90° and 180°, $|\Delta\varepsilon|$ is given by

$$\begin{cases} |\Delta\varepsilon(\ \varphi_c = 90^\circ\ )| = \left||\Delta\varphi_{A-90^\circ}| - |\Delta\varphi_{B-90^\circ}|\right| \\ |\Delta\varepsilon(\ \varphi_c = 180^\circ\ )| = \left||\Delta\varphi_{A-180^\circ}| + |\Delta\varphi_{B-180^\circ}|\right| \end{cases}. \tag{8}$$

When φ_c is 90°, $|\Delta\varphi_{A-90^\circ}|$ and $|\Delta\varphi_{B-90^\circ}|$ counteract each other, which potentially makes $|\Delta\varepsilon(\ \varphi_c = 90^\circ\ )|$ smaller. When φ_c is 180°, $|\Delta\varphi_{A-180^\circ}|$ is added by $|\Delta\varphi_{B-180^\circ}|$, which potentially increases $|\Delta\varepsilon(\ \varphi_c = 180^\circ\ )|$. Therefore, when φ_c is 90°, the practical phase difference is closer to the calculated phase difference, resulting in a better radiation pattern performance than that when φ_c is 180°. Therefore, in the design of low profile reflectarray, the chosen φ_c is supposed to make the $|\Delta\varepsilon|$ as small as possible.

C. Reflectarray Design

The proposed reflectarray consists of a waveguide acting as the feed antenna and a reflecting surface that contains 196 elements. The size of the reflecting surface is 210 mm × 210 mm. The distance from the feed antenna to the reflecting surface is 10.5 mm. The reflectarray is fed by a BJ120 waveguide.

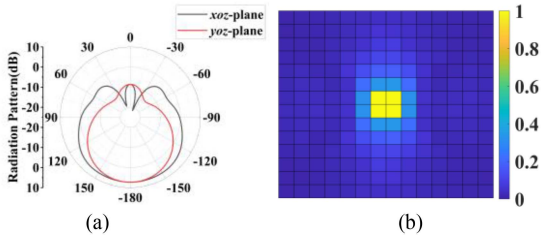

Fig. 7. (a) Radiation patterns of the feed antenna and the (b) normalized energy distribution on the reflecting surface.

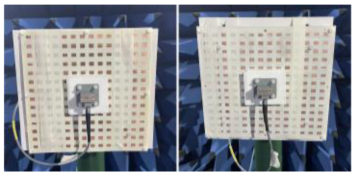

Fig. 8. Photographs of the low-profile reflectarray antenna with φ_c being (a) 90° and (b) 180°.

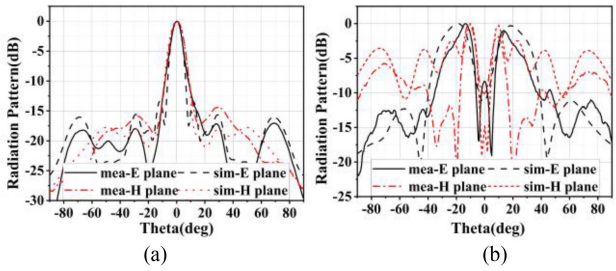

Fig. 9. Measured and simulated radiation patterns of the reflectarray at 10 GHz with φ_c being (a) 90° and (b) 180°.

The radiation patterns and the normalized energy distribution are shown in Fig. 7.

III. Prototype Development and Simulated and Measured Results

The proposed reflectarray with φ_c being 90° is simulated, fabricated, and measured. Both the simulated and measured results are shown in this section. To better illustrate the effect of the phase constant on the reflectarray, a second reflectarray with φ_c being 180° is also simulated and measured. The photographs of the reflectarrays with φ_c being 90° and 180° are shown in Fig. 8.

A. Radiation Patterns

The radiation patterns of the reflectarray with φ_c being 90° and 180° at 10 GHz in the operating band are shown in Fig. 9. The measured results are in good agreement with the simulated results. From 9.5 GHz to 10.3 GHz, the radiation patterns of the reflectarray with φ_c being 90° remain stable and undistorted. The simulated SLL1 is below −14 dB, while the measured SLL1 is below −10 dB. At 10 GHz, the simulated SLL1 is −15.7 dB, while the measured SLL1 is −14.5 dB. From 9.9 GHz to 10.1 GHz, the radiation patterns of the reflectarray with φ_c being 180° are totally distorted. At 10 GHz, the simulated SLL1 is −2.5 dB, while the measured SLL1 is below −5.8 dB.

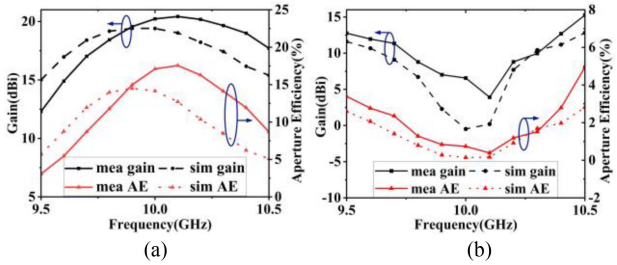

Fig. 10. Measured and simulated gain and aperture efficiency of the reflectarray with φ_c being (a) 90° and (b) 180°.

TABLE III
Comparison of Different Low-Profile Reflectarrays

Ref.	Working frequency (GHz)	F/D	H/D	Maximum Gain (dBi)	Maximum AE (%)	Bandwidth (%)
[3]	20/30	0.8	0.4	28.8/32.6	20.5/21.9	8.3/9(3-dB)
[5]	11/17	0.7	0.35	21.3/23.8	26.4/20	14/8(3-dB)
[6]	11-15	0.74	0.37	20.5–20.88	11.5–19.46	30(1-dB)
[8]	10	0.69	0.345	28.5	45	22(3-dB)
[9]	17	0.82	0.41	28.1	54.1	17(3-dB)
[11]	94.5	0.2	0.2	31.86	31.4	2.3(1-dB)
[12]	12	0.2	0.2	27.8	33.3	/
This work	10	0.05	0.05	20.42	17.55	7.73(3-dB)

B. Gain and Aperture Efficiency (AE)

Fig. 10 shows the gain and aperture efficiency of the reflectarray with φ_c being 90° and 180°. The measured results shift slightly to higher frequencies, mainly due to manufacturing and assembly errors. When φ_c is 90°, the simulated gain ranges from 15 dBi to 19.42 dBi as the frequency varies from 9.5 GHz to 10.3 GHz, peaking at 9.9 GHz, with the AE being 14.5%. The measured gain ranges from 12.3 dBi to 20.42 dBi in the working band, with the maximum measured gain occurring at 10.1 GHz and the AE being 17.55%. When φ_c is 180°, the simulated gain ranges from −0.48 dBi to 12.8 dBi, peaking at 10.5 GHz, with the AE being 2.81%. The measured gain ranges from 3.91 dBi to 15.26 dBi in the operating band. When φ_c is 90°, the radiation performance of the reflectarray is dramatically better.

Some reported low-profile reflectarrays and the reflectarray proposed in this letter are compared in Table III. As some of these low-profile reflectarrays are folded reflectarrays, the ratio of the practical height from the feed to the reflecting surface to the dimension of the reflecting surface (H/D) is also compared. The proposed reflectarray in this paper achieves the smallest F/D.

IV. Conclusion

A reflectarray with a low F/D is proposed in this letter. The performance of the reflectarray is significantly influenced by the phase constant when F/D is small. Therefore, phase constants that lead to radiation pattern deterioration should be avoided. The effect of the phase constant on the radiation pattern of the reflectarray is analyzed. Two reflectarrays with φ_c being 90° and 180° are simulated, fabricated, measured, and compared. The comparison results indicate that different φ_c values affect the radiation pattern of the reflectarray with a small F/D. The maximum measured gain of the reflectarray with φ_c being 90° is 20.42 dBi, and the maximum AE is 17.55%.

REFERENCES

[1] S. D. T. A. D. M. Pozar, "Analysis and design of a microstrip reflectarray using patches of variable size," in *Proc. Antennas Propag. Soc. Int. Symp.*, 1994, pp. 1820–1823.

[2] E. Q. R. F. Almajali and D. A. McNamara, "Angle of incidence effects in reflectarray antenna design: Making gain increases possible by including incidence angle effects," *IEEE Antennas Propag. Mag.*, vol. 58, no. 5, pp. 52–64, Oct. 2016.

[3] S. Yang, Z. Yan, M. Cai, and X. Li, "Low-profile dual-band circularly polarized antenna combining transmitarray and reflectarray for satellite communications," *IEEE Trans. Antennas Propag.*, vol. 70, no. 7, pp. 5983–5988, Jul. 2022.

[4] G.-B. Wu, S.-W. Qu, and S. Yang, "Low-profile transmitarray antenna with Cassegrain reflectarray feed," *IEEE Trans. Antennas Propag.*, vol. 67, no. 5, pp. 3079–3088, May 2019.

[5] J. Zhu, Y. Yang, S. Liao, and Q. Xue, "Dual-band antenna hybridizing folded transmitarray and folded reflectarray," *IEEE Trans. Antennas Propag.*, vol. 70, no. 4, pp. 3070–3075, Apr. 2022.

[6] S.-W. Qu, H.-X. Zhang, W.-W. Wu, P.-F. Li, S. Yang, and Z.-P. Nie, "Wideband folded reflectarray using novel elements with high orthogonal polarization isolation," *IEEE Trans. Antennas Propag.*, vol. 64, no. 7, pp. 3195–3200, 2016.

[7] Y. Shen, J. Pan, S. Xue, and S. Hu, "Wideband folded reflectarray with integrated single-layer differential slot feed," *IEEE Antennas Wireless Propag. Lett.*, vol. 23, no. 1, pp. 74–78, Jan. 2024.

[8] L. Guo, Y. Chen, and X. Chen, "A metal-only folded reflectarray antenna," *IEEE Antennas Wireless Propag. Lett.*, vol. 22, no. 6, pp. 1441–1445, Jun. 2023.

[9] A. Freni, A. Mazzinghi, and G. Carluccio, "Folded reflectarray with spherical polarizer," *IEEE Trans. Antennas Propag.*, vol. 68, no. 5, pp. 3613–3624, May 2020.

[10] G.-T. Chen, Y.-C. Jiao, G. Zhao, and C.-W. Luo, "Design of wideband high-efficiency circularly polarized folded reflectarray antenna," *IEEE Trans. Antennas Propag.*, vol. 69, no. 10, pp. 6988–6993, Oct. 2021.

[11] R. S. Hao, Y. J. Cheng, Y. F. Wu, and Y. Fan, "A W-band low-profile dual-polarized reflectarray with integrated feed for in-band full-duplex application," *IEEE Trans. Antennas Propag.*, vol. 69, no. 11, pp. 7222–7230, Nov. 2021.

[12] G.-B. Wu, S.-W. Qu, C. Ma, S. Yang, and C. H. Chan, "Reflectarray antenna design with arbitrary incident and reflection beam angle," *IEEE Trans. Antennas Propag.*, vol. 66, no. 11, pp. 5964–5973, Nov. 2018.

[13] G.-B. Wu, S.-W. Qu, S. Yang, and C. H. Chan, "Low-cost 1-D beam-steering reflectarray with $\pm 70^{\circ}$ scan coverage," *IEEE Trans. Antennas Propag.*, vol. 68, no. 6, pp. 5009–5014, Jun. 2020.

[14] W. Lin, W. Li, Y. He, L. Zhang, and S.-W. Wong, "A reflectarray with small focal diameter ratio," presented at the 16th U.K.-Europe-China Workshop on Millimetre Waves and THz Technol., Guangzhou, China, 2023.

[15] Y.-M. Cai et al., "Dual-band circularly polarized transmitarray with single linearly polarized feed," *IEEE Trans. Antennas Propag.*, vol. 68, no. 6, pp. 5015–5020, Jun. 2020.

[16] Y.-M. Cai et al., "A novel ultrawideband transmitarray design using tightly coupled dipole elements," *IEEE Trans. Antennas Propag.*, vol. 67, no. 1, pp. 242–250, Jan. 2019.

[17] W. Li, S. Gao, L. Zhang, Q. Luo, and Y. Cai, "An ultra-wide-band tightly coupled dipole reflectarray antenna," *IEEE Trans. Antennas Propag.*, vol. 66, no. 2, pp. 533–540, Feb. 2018.

[18] T. A. M. D. M. Pozar, "Analysis of a reflectarray antenna using microstrip patches of variable size," *Electron. Lett.*, vol. 29, no. 8, pp. 657–658, Apr. 1993.